Applied Numerical Mathematics 199 (2024) 153–164

Contents lists available at ScienceDirect

Applied Numerical Mathematics

journal homepage: www.elsevier.com/locate/apnum

On the formulation of energy conservation in the eeKdV equation

Anders M. Norevik *, Henrik Kalisch

Department of Mathematics, University of Bergen, Postbox 7803, 5020 Bergen, Norway

ARTICLE INFO

Article history:
Received 28 September 2022
Received in revised form 14 April 2023
Accepted 21 May 2023
Available online 25 May 2023

Keywords:
KdV equation
eeKdV equation
Surface waves
Energy conservation
Mechanical balance laws
Undular bore

ABSTRACT

The Korteweg-de Vries (KdV) equation is a well-known model equation for unidirectional shallow-water (long) surface waves. The equation includes dispersion and weak non-linearity. The derivation of the equation originates in assuming that the velocity potential takes the form of an asymptotic expansion, and applying this in the classical surface wave problem. While a typical assumption on the relative size of non-dimensional key parameters introduced in the derivation will give the KdV equation as a final result, one can change the assumption on the relative size of parameters, and end up with an equation including terms in higher orders in desired parameters. The present article presents the derivation of an extended form referred to as the eeKdV equation.

Information regarding various properties of the flow can be found by studying the derivation of the eeKdV equation itself, and some of the relations found can be used for studying the energy balance of a system modeled by the equation. In line with previous work for the KdV equation, we present here corresponding formulations of energy balance laws for an inertial reference frame, in context of the eeKdV equation. We also present a partial verification of the KdV and eeKdV energy flux expressions by looking at a far-field, uniform flow situation, as well as performing a numerical study to confirm the assumed behaviour of the error in the eeKdV energy equation in the context of a undular bore flow setup. Further, conserved integrals for the eeKdV equation are presented and numerically checked.

1. Introduction

As described in [1], the KdV equation dates back to the 1890s works of Boussinesq [13] and later Korteweg and de Vries [21]. For the KdV equation to be a reasonable model for water waves, the waves are typically required to have a limited amplitude and long wavelength when compared to the neutral (or undisturbed) fluid depth, and further the waves need to be mainly unidirectional and under negligible influence from transverse flow effects. The dimensional version of the KdV equation is given in [31] as

$$\eta_t + c_0\eta_x + \frac{3}{2}\frac{c_0}{h_0}\eta\eta_x + \frac{c_0 h_0^2}{6}\eta_{xxx} = 0\,, \tag{1.1}$$

* Corresponding author.
E-mail addresses: anders.norevik@student.uib.no (A.M. Norevik), henrik.kalisch@uib.no (H. Kalisch).

https://doi.org/10.1016/j.apnum.2023.05.020

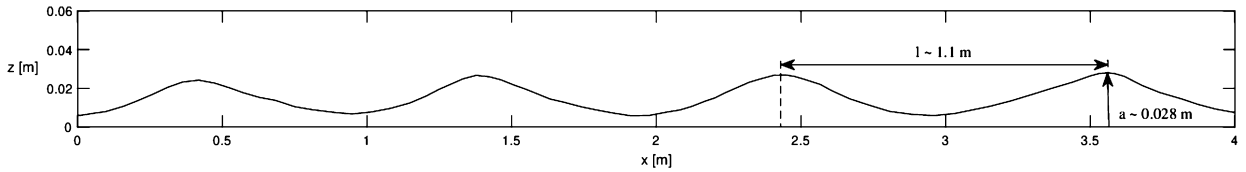

Fig. 1. Illustration of experiment 22 of Favre [18], showing that the parameter $\alpha = a/h_0$ is somewhat larger than the parameter $\beta = h_0^2/\ell^2$, justifying an assumption on the relative parameter sizes such as $\alpha^2 \approx \beta$ or $\alpha^3 \approx \beta$. Note that these are waveforms on top of a neutral fluid level of $h_0 = 0.1075$ m, and the wavelength l is approximately 1 m in this experiment.

where $\eta(x,t)$ denotes the deflection of the free surface relative to the neutral water depth h_0, g represents the acceleration by gravity, and $c_0 = \sqrt{gh_0}$ denotes the limiting speed of long waves. Note that this version of the equation is most convenient when using the equation to simulate waves on the surface of a fluid of undisturbed depth h_0. The standard form of the equation $u_t - 6uu_x + u_{xxx} = 0$ often used in the literature (see for example [17]) can be recovered by a re-scaling of the variables.

The KdV equation appears in the context of a certain scaling regime, namely the Boussinesq scaling regime. The key step here is to balance the amplitude and wavelength of the waves such that travelling-wave solutions are allowed to arise. If ℓ is used to represent a typical wavelength and a is used to represent a typical wave amplitude, the parameter $\alpha = a/h_0$ measures the relative amplitude, and $\beta = h_0^2/\ell^2$ is a measure of the relative wavenumber. For the waves to fit into the Boussinesq scaling regime, it is required that the parameters α and β are small and of comparable magnitude. Under this assumption the KdV equation will appear, as a simplified asymptotic model for the motion of waves. A more detailed explanation can be found in [1].

In the current work, we have had two key motivations to study KdV-type equations including higher order terms than the usual KdV equation itself. Firstly, as mentioned above, the Boussinesq scaling regime takes $\alpha \approx \beta$, but there may arise situations in which a more appropriate model equation may be aquired by assuming that α is somewhat larger than β, for example in experiments on undular bores done by Favre in [18]. This is shown in Fig. 1.

Under modified assumptions on the relative size of the two parameters, such as $\alpha^2 \approx \beta$ or $\alpha^3 \approx \beta$, new equations including terms to higher power in the parameter α arise during the derivation. In this paper, we are considering the relative parameter size $\alpha^3 \approx \beta$. This assumption will ultimately lead to the so-called eeKdV equation

$$\eta_t + c_0\eta_x + \frac{3}{2}\frac{c_0}{h_0}\eta\eta_x + \frac{c_0h_0^2}{6}\eta_{xxx} - \frac{3}{8}\frac{c_0}{h_0^2}\eta^2\eta_x + \frac{3}{16}\frac{c_0}{h_0^3}\eta^3\eta_x = 0\,. \tag{1.2}$$

In [1], the challenge of finding expressions for and derivations of dynamical quantities associated with the KdV equation in relevant literature is mentioned, and as such that work presented equations for mass, momentum and energy fluxes and densities in terms of the main variable η of equation (1.1). These expressions were also compared to quantities found in [5] for the steady KdV equation, and were found to agree in the limit of small α and β.

Serving as the second motivation for the current work is the observation of which energy flux relations result from applying horizontal fluid velocity expressions for respectively the KdV and eeKdV equations in the general energy flux expression for shallow water flow. In particular, while it is well known the dispersive equations develop oscillations behind the bore front (see also [23]), it was found in [5] and [30] that a small additional energy loss is required in the KdV equation which was ascribed to dissipative effects. It was shown in [3,4] that this is not necessary, and in an inviscid theory, the energy loss experienced by the shallow-water system can be accounted for by the development of oscillation in the free surface. Nevertheless, there was a small problem as the KdV equation and the Boussinesq system studied in [3,4] do not correctly reproduce the energy flux of the shallow-water system. In the current article, we put forward corresponding equations for the energy flux and energy density associated with the eeKdV equation, in terms of the main variable η of equation (1.2) It will be shown here that the energy flux in the eeKdV equation does reduce correctly to the shallow-water theory in the far field. The results of this inquiry are presented in section 4.

Given that the eeKdV equation is stated using its dimensional version (1.2), the first three conserved integrals will be

$$I_1 = \int_{-\infty}^{\infty} \eta\,dx, \quad I_2 = \int_{-\infty}^{\infty} \eta^2\,dx, \quad I_3 = \int_{-\infty}^{\infty} \left(\eta^3 - \tfrac{h_0^3}{3}\eta_x^2 - \tfrac{1}{8h_0}\eta^4 + \tfrac{3}{80h_0^2}\eta^5\right)dx. \tag{1.3}$$

It can be shown that the first integral is invariant in time t once it is observed that the eeKdV equation can be stated as

$$\frac{\partial}{\partial t}(h_0+\eta) + \frac{\partial}{\partial x}\left(c_0\eta + \frac{3}{4}\frac{c_0}{h_0}\eta^2 + \frac{c_0h_0^2}{6}\eta_{xx} - \frac{3}{24}\frac{c_0}{h_0^2}\eta^3 + \frac{3}{64}\frac{c_0}{h_0^3}\eta^4\right) = 0, \tag{1.4}$$

where the expression being differentiated with respect to time is the total depth which is here understood as a mass density, and the terms subject to the spatial differentiation is the mass flux through a unit width cross section of fluid,

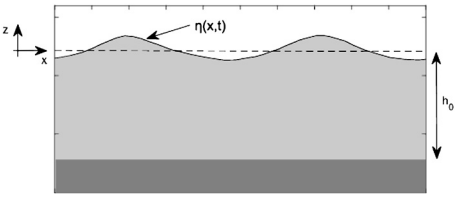

Fig. 2. The function $\eta(x,t)$ describes the free surface. We denote the undisturbed fluid depth by h_0. The x-axis ($z=0$) is aligned with the resting position of the free surface. The light gray color represents the fluid, while the dark gray color represents the bottom. The fluid density is taken to be unity.

caused by a passing surface wave. One can find invariance of the two other integrals in (1.3) by stating similar identities. For example, a firm mathematical proof is given in [11]. However, in these two latter cases, the fluxes turning up are not representative for any particular physical quantities. Nevertheless, the conserved integrals in (1.3) are useful for testing the implementation of a numerical code. Numerical tests using a Gaussian initial data are presented in section 5.

The main idea of the derivation of energy equations in this article is, as in [1], to develop an expression for energy conservation under the condition that the expression should be valid to the same order as the eeKdV equation itself is valid. In section 2, it will be shown that the non-dimensional eeKdV equation is given as

$$\tilde{\eta}_{\tilde{t}} + \tilde{\eta}_{\tilde{x}} + \frac{3}{2}\alpha\tilde{\eta}\tilde{\eta}_{\tilde{x}} + \frac{1}{6}\beta\tilde{\eta}_{\tilde{x}\tilde{x}\tilde{x}} - \frac{3}{8}\alpha^2\eta^2\eta_x + \frac{3}{16}\alpha^3\eta^3\eta_x = \mathcal{O}(\alpha^4, \alpha\beta, \beta^2) \tag{1.5}$$

The dimensional eeKdV equation (1.2) will appear after re-dimensionalization when disregarding terms of $\mathcal{O}(\alpha^4, \alpha\beta, \beta^2)$.

In section 3, it will be shown through the derivation of the energy balance law related to the eeKdV equation that if the non-dimensional energy density $\tilde{E}(\tilde{\eta})$ and non-dimensional energy flux $\tilde{q}_E(\tilde{\eta})$ are defined correctly as functions of $\tilde{\eta}$ and derivatives of $\tilde{\eta}$, and truncated at the same order as the eeKdV equations, then the relation

$$\frac{\partial}{\partial\tilde{t}}\tilde{E}(\tilde{\eta}) + \frac{\partial}{\partial\tilde{x}}\tilde{q}_E(\tilde{\eta}) = \mathcal{O}(\alpha^4, \alpha\beta, \beta^2), \tag{1.6}$$

will hold.

Note that as in [1], also in the current work the derivations are formal, and we give no mathematical proofs regarding convergence of the developed equations in the case that the parameters α and β approach zero. The primary aim of this work is to find and present an expression for the energy balance which satisfy (1.6). A proof of the validity of (1.6) is not given in the current article, but such a proof may possibly be done following the proofs given in [9,15,25] for the validity of the KdV equation itself as a model for water waves.

2. Derivation of the equation, velocity field and pressure

In this section, we derive the equations (1.2) using the method explained in detail in [31], and using the assumptions on the wavelength and amplitude outlined in the previous section. We emphasize that the relation $\alpha^3 \sim \beta$ is based on the observations and measurements on the propagation of bores in [18]. We then go on to show the equations for the velocity field and the fluid pressure, in terms of the surface deflection η.

We want to study fluid flow in a long channel of unit width. A coordinate system is positioned so that the x-axis ($z=0$) is coinciding with the undisturbed level of the free surface. The fluid domain is assumed to be infinite in positive and negative x-direction. The channel bottom is taken to be flat, and we assume that we can disregard motion of waves transverse to the x-axis. The fluid itself is taken to be inviscid and incompressible, and it is assumed that the density of the fluid is unity.

Fig. 2 shows the geometry of the problem. The general description for the surface water-wave problem is the Euler equations (in which friction is disregarded so that the no-slip boundary condition at the bottom does not apply), with kinematic and dynamic boundary conditions applied at the free surface. The unknown variables will then be the surface deflection $\eta(x,t)$, the pressure $P(x,z,t)$, horizontal fluid velocity $u_1(x,z,t)$ and vertical fluid velocity $u_2(x,z,t)$. The domain is $\left\{(x,z)\in\mathbb{R}^2 | -h_0 < z < \eta(x,t)\right\}$ which as mentioned above is considered having infinite extension in the x-direction.

The two-dimensional Euler equations on the stated domain are

$$\mathbf{u}_t + (\mathbf{u}\cdot\nabla)\mathbf{u} + \nabla P = \mathbf{g}, \tag{2.1}$$

$$\nabla\cdot\mathbf{u} = 0, \tag{2.2}$$

where the velocity field is denoted by $\mathbf{u} = (u_1, u_2)$, and $\mathbf{g} = (0, -g)$ is the gravitational acceleration associated with the body force. By the neglection of surface tension, the dynamic free-surface boundary condition requires the surface fluid pressure to equal the atmospheric pressure. Further, the kinematic free-surface boundary condition dictates that the normal velocity of the surface and the fluid velocity normal to the surface should be equal.

Under the assumption of irrotational and incompressible flow, the surface-wave problem can be recast as the Laplace equation for the velocity potential $\phi(x,z,t)$, and the surface boundary conditions will then be

$$\eta_t + \phi_x\eta_x - \phi_z = 0, \text{ on } z = \eta(x,t)\,, \tag{2.3}$$

$$\phi_t + \frac{1}{2}\left(\phi_x^2 + \phi_z^2\right) + g\eta = 0, \text{ on } z = \eta(x,t)\,. \tag{2.4}$$

With the purpose of bringing out the various sizes of the variables, we non-dimensionalize by using

$$\tilde{x} = \frac{x}{\ell}, \quad \tilde{z} = \frac{z+h_0}{h_0}, \quad \tilde{\eta} = \frac{\eta}{a}, \quad \tilde{t} = \frac{c_0 t}{\ell}, \quad \tilde{\phi} = \frac{c_0}{ga\ell}\phi$$

In the subsequent part, we are using the standard method for the development of the velocity potential ϕ in an asymptotic series. Through the use of the Laplace equation and the flat bottom boundary condition, the velocity potential will be given by

$$\tilde{\phi} = \tilde{f} - \beta\frac{\tilde{z}^2}{2}\tilde{f}_{\tilde{x}\tilde{x}} + \mathcal{O}(\beta^2), \tag{2.5}$$

in which the function $\tilde{f}(\tilde{x},\tilde{t})$ is selected so that $\tilde{f}_{\tilde{x}}$ represents the bottom horizontal fluid velocity. By the method described in Bona et al. [8] and Whitham [31], the above expression for $\tilde{\phi}$ is substituted into the surface boundary conditions. From the second free-surface boundary condition (2.4) we get the relation

$$\tilde{\eta} + \tilde{f}_{\tilde{t}} - \frac{\beta}{2}\tilde{f}_{\tilde{x}\tilde{x}\tilde{t}} + \frac{\alpha}{2}\tilde{f}_{\tilde{x}}^2 = \mathcal{O}(\alpha\beta,\beta^2). \tag{2.6}$$

By the differentiation of (2.6) with respect to $\tilde{x}$, bringing in (2.3) as the first equation, and defining $\tilde{w} = \tilde{f}_{\tilde{x}}$, we arrive at the system

$$\begin{aligned} &\tilde{\eta}_{\tilde{t}} + \tilde{w}_{\tilde{x}} + \alpha(\tilde{\eta}\tilde{w})_{\tilde{x}} + \frac{1}{6}\beta\tilde{w}_{\tilde{x}\tilde{x}\tilde{x}} = \mathcal{O}(\alpha\beta,\beta^2),\\ &\tilde{w}_{\tilde{t}} + \tilde{\eta}_{\tilde{x}} + \alpha\tilde{w}\tilde{w}_{\tilde{x}} - \frac{1}{2}\beta\tilde{w}_{\tilde{x}\tilde{x}\tilde{t}} = \mathcal{O}(\alpha\beta,\beta^2). \end{aligned} \tag{2.7}$$

From the system (2.7), various equations of KdV type can be derived through different assumptions on the relation between the non-dimensional bottom horizontal velocity $\tilde{w}$ and the surface deflection $\tilde{\eta}$. In the case of the KdV equation, it is explained in [31] how a wave solution of the system (2.7) travelling to the right requires the relation

$$\tilde{w} = \tilde{\eta} + \alpha A + \beta B + \mathcal{O}(\alpha^2,\alpha\beta,\beta^2). \tag{2.8}$$

Now, for the eeKdV equation, the corresponding required relation will be

$$\tilde{w} = \tilde{\eta} + \alpha A + \beta B + \alpha^2 C + \alpha^3 D + \mathcal{O}(\alpha^4,\alpha\beta,\beta^2). \tag{2.9}$$

To find the functions A, B, C and D we substitute (2.9) into (2.7). Using the requirement that both equations in (2.7) should give an identical equation for $\tilde{\eta}$, combined with applying the first-order derivative relation

$$\partial_{\tilde{t}}F(\tilde{\eta}) = -\partial_{\tilde{x}}F(\tilde{\eta}) + \mathcal{O}(\alpha,\beta), \tag{2.10}$$

in which F is a polynomial in $\tilde{\eta}$ and derivatives of $\tilde{\eta}$, yields

$$A = -\frac{1}{4}\tilde{\eta}^2, \quad B = \frac{1}{3}\tilde{\eta}_{\tilde{x}\tilde{x}}, \quad C = \frac{1}{8}\tilde{\eta}^3, \quad \text{and} \quad D = -\frac{5}{64}\tilde{\eta}^4.$$

Then, the requirement of equality for the equations in (2.7) results in the non-dimensional eeKdV equation

$$\tilde{\eta}_{\tilde{t}} + \tilde{\eta}_{\tilde{x}} + \frac{3}{2}\alpha\tilde{\eta}\tilde{\eta}_{\tilde{x}} + \frac{1}{6}\beta\tilde{\eta}_{\tilde{x}\tilde{x}\tilde{x}} - \frac{3}{8}\alpha^2\tilde{\eta}^2\tilde{\eta}_{\tilde{x}} + \frac{3}{16}\alpha^3\tilde{\eta}^3\tilde{\eta}_{\tilde{x}} = \mathcal{O}(\alpha^4,\alpha\beta,\beta^2), \tag{2.11}$$

and the bottom horizontal fluid velocity $\tilde{w}$ is given by

$$\tilde{w} = \tilde{\eta} - \frac{1}{4}\alpha\tilde{\eta}^2 + \frac{1}{3}\beta\tilde{\eta}_{\tilde{x}\tilde{x}} + \frac{1}{8}\alpha^2\tilde{\eta}^3 - \frac{5}{64}\alpha^3\tilde{\eta}^4 + \mathcal{O}(\alpha^4,\alpha\beta,\beta^2). \tag{2.12}$$

From (2.5) it then can be observed that the non-dimensional velocity field $(\tilde{\phi}_{\tilde{x}},\tilde{\phi}_{\tilde{z}})$ at an arbitrary non-dimensional height $\tilde{z}$ inside the fluid can be written

$$\tilde{\phi}_{\tilde{x}}(\tilde{x},\tilde{z},\tilde{t}) = \tilde{\eta} - \frac{1}{4}\alpha\tilde{\eta}^2 + \beta\Big(\frac{1}{3} - \frac{\tilde{z}^2}{2}\Big)\tilde{\eta}_{\tilde{x}\tilde{x}} + \frac{1}{8}\alpha^2\tilde{\eta}^3 - \frac{5}{64}\alpha^3\tilde{\eta}^4 + \mathcal{O}(\alpha^4, \alpha\beta, \beta^2), \tag{2.13}$$
$$\tilde{\phi}_{\tilde{z}}(\tilde{x},\tilde{z},\tilde{t}) = -\beta\tilde{z}\tilde{\eta}_{\tilde{x}} + \mathcal{O}(\alpha\beta, \beta^2).$$

By disregarding terms of fourth order in α and second order in β, and going back to dimensional variables, the eeKdV equation (1.2) will be the result. The same equation with opposite signs will account for left-travelling waves.

We now look into the expression for the pressure in the fluid. To find a pressure relation to the correct order, it is necessary to leave out the hydrostatic pressure from the calculation. For that reason, we use the dynamic pressure (also referred to as perturbation pressure) given as

$$P' = P - P_{atm} + gz.$$

The atmospheric pressure is typically much smaller than the equation's significant terms, and as such will be disregarded from this point. It can be shown, as e.g. by Stoker [29], that P' may be rewritten, by applying the Bernoulli equation, to the form

$$P' = -\phi_t - \frac{1}{2}|\nabla\phi|^2.$$

Non-dimensionalizing using $\tilde{P}' = \frac{1}{ag}P'$, and substituting equation (2.5) for ϕ gives

$$\tilde{P}' = -\tilde{f}_{\tilde{t}} + \beta\frac{\tilde{z}^2}{2}\tilde{f}_{\tilde{x}\tilde{x}\tilde{t}} - \frac{1}{2}\alpha\tilde{f}_{\tilde{x}}^2 + \mathcal{O}(\beta^2, \alpha\beta).$$

Then, following the procedure of Ali and Kalisch in [2], equation (2.6) is used to find the dynamic pressure as

$$\tilde{P}' = \tilde{\eta} + \frac{1}{2}\beta(\tilde{z}^2 - 1)\tilde{f}_{\tilde{x}\tilde{x}\tilde{t}} + \mathcal{O}(\alpha\beta, \beta^2).$$

In agreement with preceding computations, the expressions (2.9) and (2.10) are then applied, to find the expression

$$\tilde{P}' = \tilde{\eta} - \frac{1}{2}\beta(\tilde{z}^2 - 1)\tilde{\eta}_{\tilde{x}\tilde{x}} + \mathcal{O}(\alpha\beta, \beta^2). \tag{2.14}$$

In the following sections, we use (2.14) for the dynamic pressure, only truncating further if necessary in the energy balance law.

3. Energy balance

We now look into the energy balance of the fluid. Rewriting (2.1) and (2.2) in terms of the velocity potential, taking the scalar product with the fluid velocity vector and using the incompressibility conditions, an energy equation may be written in the form

$$\frac{\partial}{\partial t}\left\{\frac{1}{2}|\nabla\phi|^2 + g(z+h_0)\right\} + \nabla\cdot\left\{\left(\tfrac{1}{2}|\nabla\phi|^2 + g(z+h_0) + P\right)\nabla\phi\right\} = 0.$$

The exact details of the derivation of this balance law can be found in [16]. Integrating over the fluid depth gives

$$\frac{\partial}{\partial t}\int_{-h_0}^{\eta}\left\{\tfrac{1}{2}|\nabla\phi|^2 + g(z+h_0)\right\}dz + \frac{\partial}{\partial x}\int_{-h_0}^{\eta}\left\{\tfrac{1}{2}|\nabla\phi|^2 + g(z+h_0) + P\right\}\phi_x\,dz = 0.$$

Through a non-dimensionalization using the previously stated relations, the above equation becomes

$$\frac{\partial}{\partial\tilde{t}}\int_0^{1+\alpha\tilde{\eta}}\left\{\tfrac{\alpha^2}{2}\left(\tilde{\phi}_{\tilde{x}}^2 + \tfrac{1}{\beta}\tilde{\phi}_{\tilde{z}}^2\right) + \tilde{z}\right\}d\tilde{z}$$
$$+ \alpha\frac{\partial}{\partial\tilde{x}}\int_0^{1+\alpha\tilde{\eta}}\left\{\tfrac{\alpha^2}{2}\left(\tilde{\phi}_{\tilde{x}}^3 + \tfrac{1}{\beta}\tilde{\phi}_{\tilde{z}}^2\tilde{\phi}_{\tilde{x}}\right) + \tilde{z}\tilde{\phi}_{\tilde{x}}\right\}d\tilde{z}$$
$$+ \alpha^2\frac{\partial}{\partial\tilde{x}}\int_0^{1+\alpha\tilde{\eta}}\tilde{P}'\tilde{\phi}_{\tilde{x}}\,d\tilde{z} + \alpha\frac{\partial}{\partial\tilde{x}}\int_0^{1+\alpha\tilde{\eta}}(1-\tilde{z})\tilde{\phi}_{\tilde{x}}\,d\tilde{z} = 0.$$

By carrying out the integrals and doing the substitution of expressions for $\tilde{\phi}_{\tilde{x}}$ and $\tilde{\phi}_{\tilde{z}}$, we get

$$\frac{\partial}{\partial\tilde{t}}\Big(\frac{1}{2}+\alpha\tilde{\eta}+\alpha^2\tilde{\eta}^2+\frac{1}{4}\alpha^3\tilde{\eta}^3-\frac{3}{32}\alpha^4\tilde{\eta}^4\Big) + \frac{\partial}{\partial\tilde{x}}\Big(\alpha\tilde{\eta}+\frac{7}{4}\alpha^2\tilde{\eta}^2+\frac{1}{6}\alpha\beta\tilde{\eta}_{\tilde{x}\tilde{x}}+\frac{9}{8}\alpha^3\tilde{\eta}^3+\frac{3}{64}\alpha^4\tilde{\eta}^4\Big)=\mathcal{O}(\alpha^5,\alpha^2\beta,\alpha\beta^2).$$

Now, removing the constant term $\frac{1}{2}$ in the first bracket does not change the expression, and it is then permissible to factor out an α from both parentheses on the left, leading to

$$\alpha\frac{\partial}{\partial\tilde{t}}\Big(\tilde{\eta}+\alpha\tilde{\eta}^2+\frac{1}{4}\alpha^2\tilde{\eta}^3-\frac{3}{32}\alpha^3\tilde{\eta}^4\Big)+\alpha\frac{\partial}{\partial\tilde{x}}\Big(\tilde{\eta}+\frac{7}{4}\alpha\tilde{\eta}^2+\frac{1}{6}\beta\tilde{\eta}_{\tilde{x}\tilde{x}}+\frac{9}{8}\alpha^2\tilde{\eta}^3+\frac{3}{64}\alpha^3\tilde{\eta}^4\Big)=\mathcal{O}(\alpha^5,\alpha^2\beta,\alpha\beta^2).$$

Dividing through by α finally gives

$$\frac{\partial}{\partial\tilde{t}}\Big(\tilde{\eta}+\alpha\tilde{\eta}^2+\frac{1}{4}\alpha^2\tilde{\eta}^3-\frac{3}{32}\alpha^3\tilde{\eta}^4\Big)+\frac{\partial}{\partial\tilde{x}}\Big(\tilde{\eta}+\frac{7}{4}\alpha\tilde{\eta}^2+\frac{1}{6}\beta\tilde{\eta}_{\tilde{x}\tilde{x}}+\frac{9}{8}\alpha^2\tilde{\eta}^3+\frac{3}{64}\alpha^3\tilde{\eta}^4\Big)=\mathcal{O}(\alpha^4,\alpha\beta,\beta^2).$$

Thus by defining the non-dimensional energy density and flux according to the above expressions, we obtain the non-dimensional energy balance (1.6). Through the scaling relations $E=c_0^2h_0\tilde{E}$ and $q_E=h_0c_0^3\tilde{q}_E$, the energy density and energy flux in dimensional form are found to be

$$E=c_0^2\Big(\frac{h_0}{2}+\eta+\frac{1}{h_0}\eta^2+\frac{1}{4h_0^2}\eta^3-\frac{3}{32h_0^3}\eta^4\Big), \tag{3.1}$$

and

$$q_E=c_0^3\Big(\eta+\frac{7}{4h_0}\eta^2+\frac{h_0^2}{6}\eta_{xx}+\frac{9}{8h_0^2}\eta^3+\frac{3}{64h_0^3}\eta^4\Big). \tag{3.2}$$

Observe that the three first terms in each of the above expressions are identical to the terms found for the KdV equation in an inertial reference frame in [1], as expected. Observe also here that work done by pressure forces on the fluid is included in the energy flux.

4. Energy flux expressions in the shallow water limit

Interesting observations can be made by studying the expression for the energy flux associated to the KdV equation in the dimensional form (1.1). As shown in [1], the energy flux associated to the equation (1.1) is given by

$$q_E=c_0^3\Big(\eta+\frac{7}{4h_0}\eta^2+\frac{h_0^2}{6}\eta_{xx}\Big).$$

Here, we investigate the ramifications of the equivalent flux expression (3.2) found for the eeKdV equation in the previous section. In the context of a steady farfield flow situation, it is possible to conduct a partial algebraic verification of eeKdV energy flux expressions.

We are assuming a uniform surface displacement η and consequently zero-values of its derivatives, as well as a uniform horizontal fluid velocity over the depth of the fluid. In such a flow configuration, the expression for the dimensional energy flux across a vertical section of the flow should be the shallow water energy flux

$$q_E=\frac{1}{2}u^3h+guh^2 \tag{4.1}$$

where u denotes the horizontal fluid velocity, h is the total depth of the fluid, and g is the gravitational acceleration [3]. At this point, it is beneficial to introduce for simplicity a new method of non-dimensionalizing using

$$\tilde{x}=\frac{x}{h_0},\quad \tilde{\eta}=\frac{\eta}{h_0},\quad \tilde{t}=\sqrt{\frac{g}{h_0}}t.$$

As the horizontal fluid velocity is assumed to be uniform in the vertical coordinate direction, expressions for the bottom velocities in the KdV and eeKdV scaling regimes can be used over the entire depth of the fluid. These expressions are, in the non-dimensional variables introduced above,

$$\tilde{w}=\tilde{\eta}-\frac{1}{4}\tilde{\eta}^2 \tag{4.2}$$

in the KdV scaling regime, and

$$\tilde{w} = \tilde{\eta} - \frac{1}{4}\tilde{\eta}^2 + \frac{1}{8}\tilde{\eta}^3 - \frac{5}{64}\tilde{\eta}^4 \tag{4.3}$$

in the eeKdV scaling. Note that compared to (2.12), the derivative term disappears because of the assumed uniform η, and the two extra terms in the bottom velocity for the eeKdV is a result of the difference in the two scaling regimes. Now, by using (4.2) for the velocity in the consistently non-dimensionalized version of (4.1), as well as representing the total fluid height h by the correct non-dimensional expression in terms of $\tilde{\eta}$ we get

$$\tilde{q}_E = \frac{1}{2}\Big(\tilde{\eta} - \frac{1}{4}\tilde{\eta}^2\Big)^3(1+\tilde{\eta}) + \Big(\tilde{\eta} - \frac{1}{4}\tilde{\eta}^2\Big)(1+\tilde{\eta})^2$$

which after some calculations reduces to

$$\tilde{q}_E = \tilde{\eta} + \frac{7}{4}\tilde{\eta}^2 + \tilde{\eta}^3 - \frac{1}{8}\tilde{\eta}^4 + \dots$$

where one can observe that the two first terms carry the correct numerical coefficients when comparing with (3.2), while the numerical coefficients of the two last terms do not match their corresponding terms in (3.2).

Performing the same exercise for the eeKdV, we get first

$$\tilde{q}_E = \frac{1}{2}\Big(\tilde{\eta} - \frac{1}{4}\tilde{\eta}^2 + \frac{1}{8}\tilde{\eta}^3 - \frac{5}{64}\tilde{\eta}^4\Big)^3(1+\tilde{\eta}) + \Big(\tilde{\eta} - \frac{1}{4}\tilde{\eta}^2 + \frac{1}{8}\tilde{\eta}^3 - \frac{5}{64}\tilde{\eta}^4\Big)(1+\tilde{\eta})^2$$

which reduces to

$$\tilde{q}_E = \tilde{\eta} + \frac{7}{4}\tilde{\eta}^2 + \frac{9}{8}\tilde{\eta}^3 + \frac{3}{64}\tilde{\eta}^4 - \frac{3}{16}\tilde{\eta}^5 + \frac{9}{64}\tilde{\eta}^6 + \dots$$

which has the correct numerical coefficients for all terms in (3.2), when disregarding the derivative term. This small check confirms that, when disregarding the derivative term, the energy flux expressions found for KdV in [1] and for the eeKdV in the current work are indeed the correct ones.

Note that expressions for the KdV and eeKdV behave here in the exact same way, in the sense that an expression for the horizontal fluid velocity corrected to a given power in the parameter α inserted into the general non-dimensional shallow water energy flux expression will provide energy flux expressions for KdV and eeKdV that are correct to the same order in α as the respective horizontal velocity expressions. Note however, that the exponents in the two terms of expression (4.1) as well as the form of the non-dimensional expressions for velocity $\tilde{w}$ and the total fluid height h predicts terms in rising powers of $\tilde{\eta}$ up to and including at least $\tilde{\eta}^4$. The parameter correction order of the eeKdV scaling regime is necessary to get the correct coefficients on all terms up to and including $\tilde{\eta}^4$.

5. Numerical considerations

To acquire the results in this section, a numerical method using finite differences for spatial derivatives and a combined Adams–Bashforth/Crank–Nicolson method for the time step has been used for the numerical experiments. The method and its derivation are the same as thoroughly described in the appendix of [14], the only difference being the addition of the two new terms in the eeKdV equation, as compared to the KdV equation. The derivation of the numerical scheme used in the current work is shown in the appendix. Note that all results in this section have been found using non-dimensional equations following the scalings introduced in section 4.

As mentioned in section 1, the conserved integrals in (1.3) have been checked numerically. This was done by running a numerical simulation on a domain $\tilde{x} \in (-90, 90)$ using an initial profile given by the Gauss normal distribution function

$$\tilde{\eta}(\tilde{x}) = \frac{1}{\sigma\sqrt{2\pi}} e^{-\frac{1}{2}(\frac{\tilde{x}-\mu}{\sigma})^2}$$

with $\sigma = 1$ and $\mu = 0$. For this simulation, stepsizes $\delta\tilde{x} = 0.01$ and $\delta\tilde{t} = 0.001$ were used, and the simulation was run to 30000 timesteps. Theoretically, these integrals should be invariant in time. When calculated numerically, one have to expect some fluctuations, but the fluctuations observed are small enough to build confidence that these are indeed the correct three first conserved integrals of the eeKdV equation, where the third one is the most interesting, as it is new for this particular eeKdV equation. The results of the numerical check are given in Fig. 3. It can be seen that $\tilde{I}_1$ develops oscillations after about 10000 time steps. This is due to oscillations in $\tilde{\eta}$ hitting the left boundary. Conservation of $\tilde{I}_2$ and $\tilde{I}_3$ is better due to the fact that they contain quadratic and higher-order powers of $\tilde{\eta}$, and we have $|\tilde{\eta}| << 1$.

In order to assess the theoretical energy expressions derived in the previous section, a numerical simulation was set up. A bore was chosen as the initial condition, similarly to the work done and thoroughly described in [6]. Simply stated, the term *bore* refers to a shift between two distinct fluid depths in a free-surface flow, as illustrated in Fig. 4. A typical real-world example could be a tidal bore entering and travelling up a river outlet. Note that bore conditions require special treatment of the boundary conditions, as Dirichlet and Neumann conditions are imposed on the right, and non-zero Dirichlet conditions are imposed on the left (i.e. upstream). These issues are also explained more thoroughly in [26].

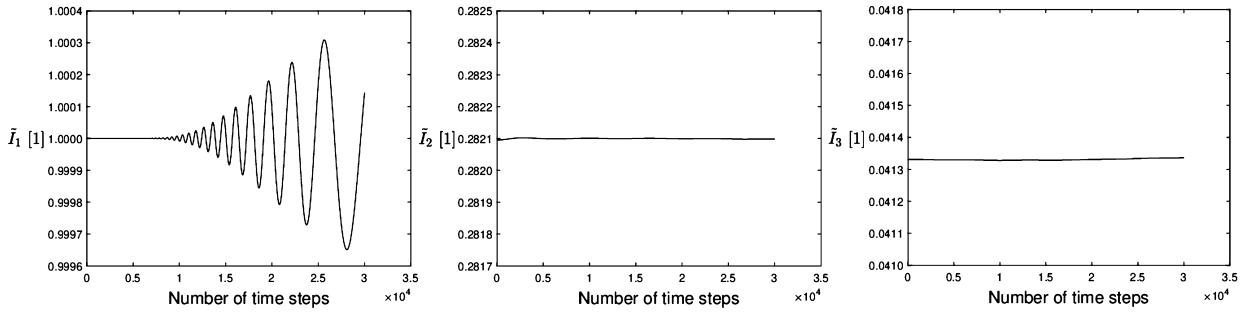

Fig. 3. Time series of numerically calculated values of non-dimensional versions of the conserved integrals given in (1.3), and in the same order. Small fluctuations observed due to normal inaccuracies in a numerical calculation.

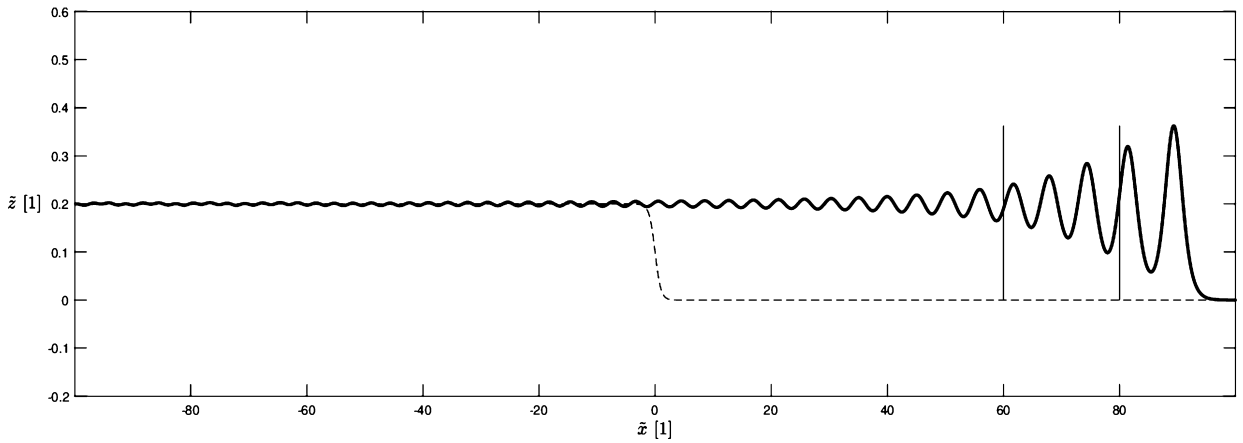

Fig. 4. Combined plot of the bore initial condition and the final surface profile for a typical numerical experiment. The initial profile is shown in dashed line, the final surface profile in a wide solid line, and the boundaries of the control volume are shown in thin solid lines. Note that the bore strength of the initial bore profile is $r = 0.2$.

We define the bore strength r as the ratio of the bore amplitude a to the neutral water depth h_0. The bore strength is illustrated for a non-dimensional case in Fig. 4.

Experience from [6] and [7] shows that numerical simulations of KdV-type and related equations combined with an initial fluid profile shaped as a sharply defined bore front will result in the appearance of a travelling train of waves where each wave is developing into approximations of solitary wave solutions of the equation, given enough time to develop. The theoretical solitary wave has a wavelength ℓ approaching infinity [31], causing the parameter $\beta = h_0^2/\ell^2$ to approach zero. As the error in the energy expression in section 3 involves terms in β, for simplification, we chose here to define a control volume $\tilde{x} \in [60, 80]$ far to the right in the spatial domain $\tilde{x} \in (-100, 100)$ in order to let the wave train leading wave have time to develop into a sufficiently close approximation to a theoretical solitary wave solution, thereby reducing the error contribution from terms involving β, and then comparing the calculation error directly to the parameter α^4, consistent with (1.6). For this series of simulations, stepsizes $\delta\tilde{x} = 0.05$ and $\delta\tilde{t} = 0.005$ were used. The simulations were run for different large enough time step numbers to allow for the leading wave to pass the right hand side control volume boundary.

The experiments show that the maximum error occurs around the time when the crest of the leading wave of the wave train reaches either the left control volume boundary or the right control volume boundary, depending on the initial bore strength r. Further, the relative size of the error compared to the fourth power of the leading wave non-dimensional amplitude α at the time of the maximum error decreases when going from small initial bore strengths to larger initial bore strengths. It is believed that this result is due to the fact that larger initial bore strengths result in a wave train where the waves develop faster into solitary waves, thereby limiting the influence of parameter β in the error term, as mentioned above. Further discussions of the role of the parameter β in errors in similar calculations can be found in [2].

To fourth order in parameter α and second order in parameter β, and on the chosen control volume, the energy balance expression takes the dimensional form

$$\frac{d}{dt}\int_{60}^{80} E(x,t)\,dx - q_E(60,t) + q_E(80,t) = 0, \tag{5.1}$$

and we have defined the non-dimensional error to be

Table 1
Shown in this table is the results of a series of numerical experiments as shown in Fig. 4. The left column states the initial bore strength r, the second column shows the non-dimensional amplitude α for the leading wave at the time of the maximum error, while the third column shows the ratio of the maximum error to α^4. Note that the error is on the order of α^4 for all cases, and less than α^4 for the last two cases.

r	α	$\frac{Err(\mathcal{E})}{\alpha^4}$
0.05	0.069	7.90
0.10	0.158	3.56
0.15	0.256	2.09
0.20	0.358	1.28
0.25	0.448	1.15
0.30	0.550	0.95
0.35	0.663	0.85

$$Err(\mathcal{E}) = \frac{1}{h_0 c_0^3} \max_t \left| \frac{d}{dt} \int_{60}^{80} E\, dx - q_E(60,t) + q_E(80,t) \right|. \tag{5.2}$$

However, for simplification, these simulations were also done using the nondimensionalizing described at the start of the section, which allows for the error to be calculated directly from non-dimensional variables as

$$Err(\mathcal{E}) = \max_{\tilde{t}} \left| \frac{d}{d\tilde{t}} \int_{60}^{80} \tilde{E}\, d\tilde{x} - \tilde{q}_E(60,\tilde{t}) + \tilde{q}_E(80,\tilde{t}) \right|. \tag{5.3}$$

It has been confirmed numerically that this method yields the same results for the error as numerically simulating (5.2) directly. The numerical experiment setup is shown in Fig. 4, and the results are given in Table 1.

6. Conclusion

Following the techniques used in [1], this article presents expressions found for the energy density E and energy flux q_E valid in the eeKdV approximation, by motivations from experimentally observed size relations between key parameters α and β, as well as differences for KdV and eeKdV scaling regimes horizontal velocity expressions when applied in a far-field steady uniform flow context.

Numerical experiments confirm that the error in the eeKdV energy balance using the derived expressions is on the order anticipated from the theoretical derivations, and the error is within the limit given by the relevant power of the parameter α as long as the waves are allowed to develop into sufficiently close approximations of theoretical solitary waves before the maximum error occurs, presumably because the parameter β, and consequently its influence in the energy expressions, approaches zero in the context of such waves.

As previously pointed out, it should be noted that a formal procedure to find the expressions for the energy density and energy flux has been used. As such, the results given here may provide the starting point in the search for a mathematical method to prove that the energy balance (1.6) is valid to identical order and over identical time scales as the eeKdV equation (1.2) itself. It is not quite obvious how to utilize available methods of mathematical justification for various model equations to justify the associated energy balance law found here. Some results in this direction can be found in [20], but much more remains to be done.

We should also mention that while the relation $\alpha^3 \sim \beta$ was found from the experiments of Favre [18], other scaling relations can be relevant. In some cases, the relation $\alpha^2 \sim \beta$ would be more appropriate, leading to the extended KdV equation (eKdV) [27,28] or variants thereof [24]. On the other hand, there has been recent work on the fully dispersive scaling regime associated to the Whitham equation [31] (see [19,22] and references therein).

Appendix - Numerical method for the eeKdV equation

Finite-difference methods applied to the spatial derivatives, as well as a combination of the Adam-Bashforth and Crank-Nicolson methods for the timestep, constitute the numerical procedure to find an approximation of the solution $\eta(x,t)$ in (1.2). The method has been used before in e.g. [7,14,26], but in those works it was applied to variants of the KdV equation. For a KdV equation having common terms with the eeKdV equation studied in the current work, the method is described in the appendix of [14]. The difference in the current work is solely the inclusion of the two extra terms in the eeKdV equation in the derivation of the numerical scheme. Nevertheless, we include the main steps of the derivation here for clarity.

The imposing of boundary conditions are required for a proper definition of a numerical discretization. We specialize here to a bore case, as shown in Fig. 4. At far-field locations far away from the bore front on the chosen spatial domain, the surface deflection η will approximate α to the left and 0 to the right. For a sufficiently sizable spatial domain, the above-mentioned boundary conditions will be exact to machine precision. Further, we need to define a Neumann boundary condition for the right far-field boundary, as described in e.g. [12]. Utilizing a homogenous Neumann condition together with the described Dirichlet boundary conditions, we now have an initial/boundary-value problem given as

$$\begin{aligned} \eta_t + \eta_x + \tfrac{3}{4}(\eta^2)_x - \tfrac{3}{24}(\eta^3)_x + \tfrac{3}{64}(\eta^4)_x + \tfrac{1}{6}\eta_{xxx} = 0, x \in (-l, l),\, t \geq 0, \\ \eta(x,0) = \eta_0(x), \\ \eta(-l,t) = \alpha, \\ \eta(l,t) = 0, \\ \eta_x(l,t) = 0. \end{aligned} \tag{6.1}$$

For the bore case, the initial profile is $\eta_0(x) = \frac{1}{2}a_0\big[1 - \tanh(kx)\big]$, in which the parameter k controls the slope of the initial front of the bore, where larger values will give a steeper bore front. As in [7], we choose here to use $k = 1$.

At this point it is advantageous to rephrase the problem so that the boundary conditions will be homogenous. We achieve this by introducing an auxiliary function

$$\zeta(x,t) \equiv \eta(x,t) - \eta_0(x). \tag{6.2}$$

With ζ, we can now rewrite the problem in terms of an inhomogeneous equation having forcing represented by ζ and η_0, while the boundary conditions and initial conditions are now homogenous. Recast in terms of ζ, the equation becomes

$$\begin{aligned} &\zeta_t + \zeta_x + \tfrac{3}{4}(\zeta^2)_x + \tfrac{3}{2}(\zeta\eta_0)_x - \tfrac{3}{8}(\zeta^2\eta_0)_x - \tfrac{3}{8}(\zeta\eta_0^2)_x - \tfrac{3}{24}(\zeta^3)_x \\ &\quad + \tfrac{3}{16}(\zeta^3\eta_0)_x + \tfrac{3}{16}(\zeta\eta_0^3)_x + \tfrac{9}{32}(\zeta^3\eta_0^2)_x + \tfrac{3}{64}(\zeta^4)_x + \tfrac{1}{6}\zeta_{xxx} = -F, x \in (-l, l),\, t \geq 0, \end{aligned}$$

where

$$F \equiv \eta_0' + \tfrac{3}{2}\eta_0\eta_0' - \tfrac{3}{8}(\eta_0^2\eta_0') + \tfrac{3}{16}(\eta_0^3\eta_0') + \tfrac{1}{6}\eta_0''',$$

while also imposing homogenous boundary and initial conditions. Discretization of the spatial domain $[-l, l]$ is done utilizing a confined selection of grid points, $\{x_j\}_{j=0}^{N} \subset [-l, l]$, where $x_0 = -l$ and $x_N = l$, while $\delta x = 2l/N$ gives the spacing between two adjacent points on the grid. For the temporal domain, a uniform discretization is carried out by using $t_n = n\delta t$, for which t_0 equals zero. In the introduced notation, the approximation of the exact value of the function $\zeta(x,t)$ at time t_n and gridpoint x_j is represented by $v_j^n \approx \zeta(x_j, t_n)$.

As can be seen above, special interest is associated with the first and the third derivatives in the spatial discretization. The values of these derivatives at a grid point x_j are estimated using the central difference formulas

$$\zeta_x(x_j,t) \approx \frac{v_{j+1} - v_{j-1}}{2\delta x} \tag{6.3}$$

and

$$\zeta_{xxx}(x_j,t) \approx \frac{v_{j+2} - 2v_{j+1} + 2v_{j-1} - v_{j-2}}{2\delta x^3}. \tag{6.4}$$

Due to the enforcing of Dirichlet boundary conditions $v_0 = 0$ and $v_N = 0$, we can solve the equation for spatial grid points $\{x_j\}_{j=1}^{N-1}$, leaving only two grid points where the validity of the approximation of the third derivative breaks down. From the Neumann boundary condition in addition to the central difference approximation, we get $(v_{N+1} - v_{N-1})/2\delta x = 0$ with the implication $v_{N+1} = v_{N-1}$, which makes it possible to use the below expression to approximate the third derivative at the point x_{N-1}

$$\zeta_{xxx}(x_{N-1},t) \approx \frac{v_{N+1} - 2v_N + 2v_{N-2} - v_{N-3}}{2\delta x^3} = \frac{v_{N-1} + 2v_{N-2} - v_{N-3}}{2\delta x^3}. \tag{6.5}$$

The absence of a Neumann boundary condition at the left-hand side of the domain enables us to calculate an approximation of the third spatial derivative at the grid point x_1 by forward difference as given below:

$$\zeta_{xxx}(x_1,t) \approx \frac{-v_4 + 6v_3 - 12v_2 + 10v_1 - 3v_0}{2\delta x^3}. \tag{6.6}$$

Employing the difference expressions (6.3), (6.4), (6.5) and (6.6) at grid points throughout the entire domain results in the following discrete differentiation matrices D_1 and D_3:

$$D_1 = \frac{1}{2\delta x}\begin{pmatrix} 0 & 1 & 0 & & & \cdots & 0 \\ -1 & 0 & 1 & 0 & & & \vdots \\ 0 & -1 & 0 & 1 & 0 & & \\ \vdots & & & \ddots & & & \\ 0 & \cdots & & & & 0 & 1 \\ 0 & \cdots & & & & -1 & 0 \end{pmatrix}, \qquad D_3 = \frac{1}{2\delta x^3}\begin{pmatrix} 10 & -12 & 6 & -1 & 0 & \cdots & 0 \\ 2 & 0 & -2 & 1 & 0 & \cdots & 0 \\ -1 & 2 & 0 & -2 & 1 & 0 & \\ 0 & -1 & 2 & & \ddots & & \\ \vdots & & & \ddots & & \ddots & 1 \\ & & & & \ddots & 0 & -2 \\ 0 & & \cdots & & -1 & 2 & 1 \end{pmatrix}.$$

We proceed now by using a Crank-Nicolson scheme for the linear terms in the equation's right-hand side, while we apply an Adams-Bashforth scheme for the non-linear terms. By doing this, we aquire the following difference equation for vector $\mathbf{v}^{n+1}$:

$$\begin{aligned} \frac{\mathbf{v}^{n+1}-\mathbf{v}^n}{\delta t} = &-\tfrac{3}{4}D_1\Big[\tfrac{3}{2}\Big((\mathbf{v}^n)^2 + 2\mathbf{v}^n\eta_{\mathbf{0}} + \tfrac{1}{16}(\mathbf{v}^n)^4 - \tfrac{1}{6}(\mathbf{v}^n)^3 + \tfrac{1}{4}(\mathbf{v}^n)^3\eta_{\mathbf{0}} \\ &+ \tfrac{3}{8}(\mathbf{v}^n)^3{\eta_{\mathbf{0}}}^2 - \tfrac{1}{2}(\mathbf{v}^n)^2\eta_{\mathbf{0}} - \tfrac{1}{2}\mathbf{v}^n\eta_{\mathbf{0}}^{\mathbf{2}} + \tfrac{1}{4}\mathbf{v}^n\eta_{\mathbf{0}}^{\mathbf{3}}\Big) \\ &+ \tfrac{1}{2}\Big((\mathbf{v}^{n-1})^2 + 2\mathbf{v}^{n-1}\eta_{\mathbf{0}} + \tfrac{1}{16}(\mathbf{v}^{n-1})^4 - \tfrac{1}{6}(\mathbf{v}^{n-1})^3 + \tfrac{1}{4}(\mathbf{v}^{n-1})^3\eta_{\mathbf{0}} \\ &+ \tfrac{3}{8}(\mathbf{v}^{n-1})^3{\eta_{\mathbf{0}}}^2 - \tfrac{1}{2}(\mathbf{v}^{n-1})^2\eta_{\mathbf{0}} - \tfrac{1}{2}\mathbf{v}^{n-1}\eta_{\mathbf{0}}^{\mathbf{2}} + \tfrac{1}{4}\mathbf{v}^{n-1}\eta_{\mathbf{0}}^{\mathbf{3}}\Big)\Big] \\ &- \tfrac{1}{2}\Big[D_1\Big(\mathbf{v}^{n+1}+\mathbf{v}^n\Big) + \tfrac{1}{6}D_3\Big(\mathbf{v}^{n+1}+\mathbf{v}^n\Big)\Big] - \mathbf{F}, \end{aligned}$$

for which $\mathbf{v}^n = (v_1^n, v_2^n, ..., v_{N-1}^n)^T$, $\eta_{\mathbf{0}} = (\eta_0(x_1), \eta_0(x_2), ..., \eta_0(x_{N-1}))^T$ and $\mathbf{F} = (F(x_1), F(x_2), ..., F(x_{N-1}))^T$. The above $n \times n$-system of equations is readily solved for $\mathbf{v}^{n+1}$, and the requirement is just three multiplications by sparse matrices to progress the numerical approximative solution one step forward in time.

Through an introduction of the matrix $E = (I + \frac{\delta t}{2}D_1 + \frac{\delta t}{12}D_3)$, the equation above can be rewritten as

$$\begin{aligned} \mathbf{v}^{n+1} = &E^{-1}\Big[I - \tfrac{\delta t}{2}D_1 - \tfrac{\delta t}{12}D_3\Big]\mathbf{v}^n \\ &- \tfrac{3\delta t}{4}E^{-1}D_1\Big[\tfrac{3}{2}\Big((\mathbf{v}^n)^2 + 2\mathbf{v}^n\eta_{\mathbf{0}} + \tfrac{1}{16}(\mathbf{v}^n)^4 - \tfrac{1}{6}(\mathbf{v}^n)^3 + \tfrac{1}{4}(\mathbf{v}^n)^3\eta_{\mathbf{0}} \\ &+ \tfrac{3}{8}(\mathbf{v}^n)^3{\eta_{\mathbf{0}}}^2 - \tfrac{1}{2}(\mathbf{v}^n)^2\eta_{\mathbf{0}} - \tfrac{1}{2}\mathbf{v}^n\eta_{\mathbf{0}}^{\mathbf{2}} + \tfrac{1}{4}\mathbf{v}^n\eta_{\mathbf{0}}^{\mathbf{3}}\Big) \\ &+ \tfrac{1}{2}\Big((\mathbf{v}^{n-1})^2 + 2\mathbf{v}^{n-1}\eta_{\mathbf{0}} + \tfrac{1}{16}(\mathbf{v}^{n-1})^4 - \tfrac{1}{6}(\mathbf{v}^{n-1})^3 + \tfrac{1}{4}(\mathbf{v}^{n-1})^3\eta_{\mathbf{0}} \\ &+ \tfrac{3}{8}(\mathbf{v}^{n-1})^3{\eta_{\mathbf{0}}}^2 - \tfrac{1}{2}(\mathbf{v}^{n-1})^2\eta_{\mathbf{0}} - \tfrac{1}{2}\mathbf{v}^{n-1}\eta_{\mathbf{0}}^{\mathbf{2}} + \tfrac{1}{4}\mathbf{v}^{n-1}\eta_{\mathbf{0}}^{\mathbf{3}}\Big)\Big] \\ &- \delta t E^{-1}\mathbf{F}. \end{aligned}$$

In general, and as can be observed from the above expression, this scheme needs values of the function $\mathbf{v}$ from the two preceding time steps to advance forward in time. As mentioned in [14], a possible technique to solve this is to apply the forward Euler method for the non-linear terms for the initial step forward in time. However, in the current work we have solved this by using a "work-around" in the code in which we set both $\mathbf{v}^n$ and $\mathbf{v}^{n-1}$ to be $\mathbf{0}$ at the start of the numerical simulation.

In conclusion of this appendix, it should also be mentioned that all terms in the numerical code for (1.2) have been tested through running convergence checks of the generalized KdV equation (GKdV)

$$\eta_t + \eta^p\eta_x + \epsilon\eta_{xxx} = 0\,,$$

with $\epsilon = 1$ and $p = 1, 2$ and 3, using analytical solutions given in [10]. All checks confirm that the numerical scheme exhibits second order accuracy in both the spatial step and the time step respectively.

References

[1] A. Ali, H. Kalisch, On the formulation of mass, momentum and energy conservation in the KdV equation, Acta Appl. Math. 133 (2014) 113–131.
[2] A. Ali, H. Kalisch, Mechanical balance laws for Boussinesq models of surface water waves, J. Nonlinear Sci. 22 (2012) 371–398.
[3] A. Ali, H. Kalisch, Energy balance for undular bores, C. R., Méc. 338 (2010) 67–70.
[4] A. Ali, H. Kalisch, A dispersive model for undular bores, Anal. Math. Phys. 2 (2012) 347–366.

[5] T.B. Benjamin, M.J. Lighthill, On cnoidal waves and bores, Proc. R. Soc. Lond. Ser. A 224 (1954) 448–460.
[6] M. Bjørkavåg, H. Kalisch, Wave breaking in Boussinesq models for undular bores, Phys. Lett. A 375 (2011) 1570–1578.
[7] M. Bjørnestad, H. Kalisch, M. Abid, C. Kharif, M. Brun, Wave breaking in undular bores with shear flows, Water Waves 3 (2021) 473–490.
[8] J.L. Bona, M. Chen, J.-C. Saut, Boussinesq equations and other systems for small-amplitude long waves in nonlinear dispersive media. I: Derivation and linear theory, J. Nonlinear Sci. 12 (2002) 283–318.
[9] J.L. Bona, T. Colin, D. Lannes, Long wave approximations for water waves, Arch. Ration. Mech. Anal. 178 (2005) 373–410.
[10] J.L. Bona, V.A. Dougalis, O.A. Karakashian, W.R. McKinney, Computations of blow-up and decay for periodic solutions of the generalized Korteweg-de Vries-Burgers equation, Appl. Numer. Math. 10 (1992) 335–355.
[11] J.L. Bona, R. Smith, The initial value problem for the Korteweg-de Vries equation, Proc. R. Soc. Lond. Ser. A 278 (1975) 555–601.
[12] J.L. Bona, S.M. Sun, B.-Y. Zhang, A nonhomogeneous boundary-value problem for the Korteweg-de Vries equation posed on a finite domain, Commun. Partial Differ. Equ. 28 (2003) 1391–1436.
[13] J. Boussinesq, Théorie des ondes et des remous qui se propagent le long d'un canal rectangulaire horizontal, en communiquant au liquide contenu dans ce canal des vitesses sensiblement pareilles de la surface au fond, J. Math. Pures Appl. 17 (1872) 55–108.
[14] M.K. Brun, H. Kalisch, Convective wave breaking in the KdV equation, Anal. Math. Phys. 8 (2018) 57–75.
[15] W. Craig, An existence theory for water waves and the Boussinesq and Korteweg-de Vries scaling limits, Commun. Partial Differ. Equ. 10 (1985) 787–1003.
[16] G.D. Crapper, Introduction to Water Waves, Ellis, Horwood, 1984.
[17] P.G. Drazin, R.S. Johnson, Solitons: an Introduction, Cambridge University Press, Cambridge, 1989.
[18] H. Favre, Ondes de Translation, Dunod, Paris, 1935.
[19] M.V. Flamarion, Solitary wave collisions for the Whitham equation, Comput. Appl. Math. 41 (2022) 356.
[20] S. Israwi, H. Kalisch, A mathematical justification of the momentum density function associated to the KdV equation, C. R. Math. 395 (2021) 39–45.
[21] D.J. Korteweg, G. de Vries, On the change of form of long waves advancing in a rectangular channel and on a new type of long stationary wave, Philos. Mag. 39 (1895) 422–443.
[22] D. Moldabayev, H. Kalisch, D. Dutykh, The Whitham equation as a model for surface water waves, Physica D 309 (2015) 99–107.
[23] P.G. Peregrine, Calculations of the development of an undular bore, J. Fluid Mech. 25 (1966) 321–330.
[24] P. Rozmej, A. Karczewska, E. Infeld, Superposition solutions to the extended KdV equation for water surface waves, Nonlinear Dyn. 91 (2018) 1085–1093.
[25] G. Schneider, C.E. Wayne, The long-wave limit for the water wave problem. I. The case of zero surface tension, Commun. Pure Appl. Math. 53 (2000) 1475–1535.
[26] J.O. Skogestad, H. Kalisch, A boundary value problem for the KdV equation: comparison of finite-difference and Chebyshev methods, Math. Comput. Simul. 80 (2009) 151–163.
[27] A.V. Slunyaev, E.N. Pelinovsky, Role of multiple soliton interactions in the generation of rogue waves: the modified Korteweg-de Vries framework, Phys. Rev. Lett. 117 (2016) 214501.
[28] A.V. Slunyaev, T.V. Tarasova, Statistical properties of extreme soliton collisions, Chaos, Interdiscip. J. Nonlinear Sci. 32 (2022) 101102.
[29] J.J. Stoker, Water Waves, The Mathematical Theory with Applications, Pure and Applied Mathematics, vol. 4, Interscience Publishers, New York, 1957.
[30] B. Sturtevant, Implications of experiments on the weak undular bore, Phys. Fluids 6 (1965) 1052–1055.
[31] G.B. Whitham, Linear and Nonlinear Waves, Wiley, New York, 1974.